

MOL Manuscript #103200

Title page

Synthesis and Evaluation of Potent KCNQ2/3-specific Channel Activators

Manoj Kumar, Nicholas Reed, Ruiting Liu, Elias Aizenman, Peter Wipf and Thanos Tzounopoulos

Department of Otolaryngology, University of Pittsburgh School of Medicine, Pittsburgh, Pennsylvania 15261 (M.K., T.T); Department of Chemistry, University of Pittsburgh, Pittsburgh, Pennsylvania 15260 (N.R., R.L., PW); Department of Neurobiology, University of Pittsburgh, Pittsburgh, Pennsylvania 15261 (E.A., T.T.) and Pittsburgh Institute for Neurodegenerative Diseases, University of Pittsburgh School of Medicine (E.A).

MOL Manuscript #103200

Running title page

Novel KCNQ2/3 channel activators

Corresponding authors:

Thanos Tzounopoulos, Department of Otolaryngology and Department of Neurobiology,
University of Pittsburgh, Pittsburgh, Pennsylvania 15261

Email: thanos@pitt.edu

Peter Wipf, Department of Chemistry, University of Pittsburgh, Pittsburgh, Pennsylvania 15260

Email: pwipf@pitt.edu

Number of Text pages: 36

Number of Tables: 0

Number of Figures: 9

Number of References: 43

Number of words in Abstract: 133

Number of words in Introduction: 709

Number of words in Discussion: 732

MOL Manuscript #103200

Abbreviations: ADME/tox, Absorption, distribution, metabolism, excretion/ toxicity; Cbz, benzyloxycarbonyl; CHO, chinese hamster ovary; DMSO, dimethyl sulfoxide; DIPEA, di-*isopropylethylamine*; EGTA, ethylene glycol-bis(β -aminoethyl ether)-N,N,N',N'-tetraacetic acid; HEPES, N-(2-hydroxyethyl)-1-piperazineethanesulfonic acid; Kv, voltage-gated potassium channel; PTSA, *para*-toluenesulfonic acid; SAR, structure-activity relationship; S_NAr, nucleophilic aromatic substitution.

Abstract

KCNQ channels are voltage-gated, non-inactivating potassium ion channels, and their down-regulation has been implicated in several hyperexcitability-related disorders, including epilepsy, neuropathic pain and tinnitus. Activators of these channels reduce the excitability of central and peripheral neurons, and, as such, have therapeutic utility. Here, we synthetically modified several moieties of the KCNQ2-5 channel activator retigabine, an FDA approved anti-convulsant. By introducing a CF₃-group at the 4-position of the benzylamine moiety, combined with a fluorine atom at the 3-position of the aniline ring, we generated RL648_81, a new KCNQ2/3-specific activator (EC₅₀ 190 nM) that is >15 times more potent and also more selective than retigabine (EC₅₀ 3.3 μM). We suggest that RL648_81 is a promising clinical candidate for treating or preventing neurological disorders associated with neuronal hyperexcitability.

Introduction

Epilepsy is the most common neuronal hyperexcitability disorder, affecting 1% of the world population. This neurological condition is generally managed with sodium channel blockers or GABA receptor agonists (Bialer et al., 2010; Bialer and White, 2010). Although there are several drugs in clinical use with distinct mechanism of action, unfortunately approximately 30% of patients do not respond to these agents (Brodie, 2010; Sharma et al., 2015). Thus, there is an urgent need for drug development to broaden the treatment options.

KCNQ (or Kv7) channels play a critical role in maintaining neuronal excitability and have recently emerged as a potential target for the prevention and treatment of epilepsy and other hyperexcitability-related disorders, including neuropathic pain and tinnitus (Brown and Passmore, 2009; Gribkoff, 2008; Grunnet et al., 2014; Miceli et al., 2008; Wickenden and McNaughton-Smith, 2009; Wulff et al., 2009; Li et al., 2013). KCNQ channels are voltage-gated, non-inactivating potassium ion channels (Brown and Adams, 1980). These channels are open at resting membrane potentials and function as a ‘brake’ on the excitability of central and peripheral neurons (Robbins, 2001). The KCNQ family comprises of five subunits (KCNQ1-5): KCNQ2-5 are confined to the nervous system including brainstem and inner ear whereas KCNQ1 is limited to the heart and peripheral epithelial and smooth muscle cells (Howard et al., 2007). Genetic mutations in either KCNQ2 or KCNQ3 subunits are linked to benign familial neonatal convulsions, whereas noise-induced reduction in KCNQ2/3 channel current leads to development of tinnitus in mice (Biervert et al., 1998; Jentsch, 2000; Li et al., 2013; Li et al., 2015). Moreover, pathological reduction in KCNQ2/3 channel activity is involved in different classes of seizures, neuropathic pain, migraine, anxiety, attention deficient-hyperactivity disorder, schizophrenia, mania and bipolar disease (Grunnet et al., 2014; Hansen et al., 2008;

Munro and Dalby-Brown, 2007). As a result, KCNQ channel activators, which lead to the opening of these channels at more hyperpolarized potentials, have recently been employed to treat or prevent epilepsy (Gribkoff, 2008; Miceli et al., 2008; Xiong et al., 2008).

Several Kv7 channel openers are under active development for the management of hyperexcitability disorders (Dalby-Brown et al., 2013; Davoren et al., 2015; Grunnet et al., 2014; Stott et al., 2014). Retigabine, which activates all KCNQ2-5 channels, is the only FDA approved anti-convulsant KCNQ activator (Gunthorpe et al., 2012; Tatulian et al., 2001). However, recent data showed severe side effects associated with retigabine, including urinary retention, blue skin discoloration and retinal abnormalities (Jankovic and Ilickovic, 2013). As a result, the FDA limited its use to patients who have not responded to alternative treatments. The undesirable side effects are likely due to the poor selectivity of retigabine among KCNQ2-5 channels as well as metabolic degradation products of its aniline ring. For example, retigabine activates KCNQ4 and KCNQ5, which are not involved in the pathology of hyperexcitability-related disorders. KCNQ4 is the primary potassium channel in the smooth muscle of the bladder, where it regulates contractility (Greenwood and Ohya, 2009; Jentsch, 2000). Activation of KCNQ4 leads to membrane hyperpolarization and results in significantly reduced contractility, which may be the cause for urinary retention associated with the use of retigabine. Moreover, a form of dominant deafness arises from loss of function of KCNQ4 (Kharkovets et al., 2000), and therefore opening of these channels may affect hearing. In addition to expression in the CNS, KCNQ4 and KCNQ5 are also found in skeletal muscle (Iannotti et al., 2013; Iannotti et al., 2010; Jentsch, 2000). Accordingly, there is an urgent need for the development of potent and selective KCNQ2/3 channel activators, which, unlike retigabine, do not activate KCNQ4 and KCNQ5 channels.

MOL Manuscript #103200

To achieve this aim, we synthesized and evaluated several novel KCNQ2/3-specific channel activators. To maximize potency, we manipulated the different chemical components or “zones” of retigabine (Figure 1). Particularly, by introducing a CF₃-group in zone 1 at the 4-position of the benzylamine moiety, combined with a fluorine atom in zone 2 at the 3-position of the aniline ring, we generated RL648_81, a new KCNQ2/3-specific activator that is 3 times more potent and also more selective than SF0034, a recently described retigabine analog with increased potency and selectivity for KCNQ2/3 channels (Kalappa et al., 2015). We propose that RL648_81 is a promising clinical candidate for the treatment or prevention of hyperexcitability-related neurological disorders.

Materials and Methods

Constructs and Chemicals. The KCNQ2, KCNQ3, KCNQ4, KCNQ5 and KCNQ2 (W236L) constructs, as well as the PIPKI γ 90 plasmid used in this study have been described previously (Soh and Tzingounis, 2010; Kalappa et al., 2015) and were generously provided by Dr. Anastassios Tzingounis (University of Connecticut, Connecticut, USA). Buffers and salts were purchased from Sigma-Aldrich (St. Louis, Missouri, USA). Compounds stock solutions (20 mM) were made in DMSO. All stock solutions were stored at -20 °C. On the day of experiment, fresh working drug concentrations were prepared from stock solutions by dissolving them in physiological buffer solution.

Cell Culture and Transfection. Chinese hamster ovary (CHO) cells were plated on glass coverslips in 35-mm culture dishes and were incubated and maintained at 37 °C in a humidified incubator with 5% CO₂. To get heterologous KCNQ2/3 configuration, CHO cells were transfected with human KCNQ2 and KCNQ3 subunits cDNA in a 1:1 (0.5 μ g : 0.5 μ g) ratio with 0.5 μ g of GFP plasmid using *lipofectamine transfection reagent* (Thermo Fisher Scientific, MA, USA) and used for recording within 24-72 h of post transfection. For homomeric KCNQ4 and KCNQ5 channels, 1 μ g of plasmid cDNA was used. To record robust KCNQ5 currents, we cotransfected KCNQ5 with pIRES-dsRed-PIPKI γ 90. PIPKI γ 90 increases KCNQ channel open probability (Li et al., 2005).

Whole cell patch clamp electrophysiology. We used whole-cell patch clamp electrophysiology used to assess effects of retigabine and synthesized compounds on KCNQ channel currents. We conducted electrophysiology experiments at room temperature (22-25 °C). Patch pipettes of borosilicate glass (BF150-110-10; Sutter Instrument Company, Novato, CA) were pulled to a tip resistance of 4–6 M Ω . Patch pipettes were filled with a solution consisting of (in mM): 132 K-

gluconate, 10 KCl, 4 Mg•ATP, 20 HEPES, and 1 EGTA•KOH, pH 7.2–7.3. Coverslips containing cultured cells were placed in the recording chamber on the stage of an inverted light microscope and superfused continuously with an external solution consisting of (in mM): 144 NaCl, 2.5 KCl, 2.25 CaCl₂, 1.2 MgCl₂, 10 HEPES, and 22 D-glucose, pH 7.2–7.3. Osmolarity was adjusted to 300–305 mOsm and pH to 7.2–7.3 with NaOH. Cells were clamped at -85 mV and currents were elicited by 1 s depolarization potentials, in 10 mV increments, from -105 to +15 mV followed by a return step to -70 mV. Currents elicited by each voltage step were measured and used to generate the conductance-voltage (G-V) curves as described in the figure legends. These values are adjusted for the calculated junction potential, which was -15 mV. Series resistance was compensated by 75%. To quantify the potency of the tested compounds, we measured the shift in $V_{1/2}$ at increasing concentrations and used a Hill equation fit to calculate their EC₅₀, which is the concentration of the compound that produces a half-maximal shift in $V_{1/2}$. Data were acquired through an Axopatch 200 amplifier (Molecular Devices, Sunnyvale, CA), low-pass filtered at 2 kHz, sampled at 10 kHz using pClamp 10 data acquisition system.

Data analysis and statistics. We used the Boltzmann function to fit the conductance–voltage curves and determine the maximal conductance (G_{max}) and half-maximal activation voltage ($V_{1/2}$) of KCNQ currents, where $G = G_{max}/[1 + e^{\{-(V - V_{1/2})/k\}}]$ and k is the slope factor. To calculate the dependence of the shift in $V_{1/2}$ with the concentration of different KCNQ channel activators, we measured the $V_{1/2}$ of KCNQ2/3 currents in presence of various concentrations of compounds (100 nM–30 μ M). We then fitted the agonist dependence of the shift of the $V_{1/2}$ obtained by different concentrations with a Hill equation, where $\Delta V_{1/2} = V_{1/2} \max * [\text{activator}]^n / ([\text{activator}]^n + EC_{50}^n)$. $\Delta V_{1/2}$ is the change in $V_{1/2}$ caused by the activator, EC₅₀ is the concentration of the KCNQ channel activator that causes 50% of the maximal effect in $V_{1/2}$, n is

MOL Manuscript #103200

the Hill coefficient, and [activator] is the concentration of KCNQ activator. All data are presented as mean values \pm S.E.M. Statistical significance between control and test conditions was determined using Student's *t*-test (paired or unpaired) and one-way analysis of variance. Tukey-Kramer *post hoc* test for multiple comparisons was performed as needed. Data analysis and statistical tests were performed using GraphPad Prism version 6 and OriginLab 2015.

Results

Retigabine and its derivative SF0034 shift the voltage dependent opening of KCNQ channels towards more hyperpolarized potentials, leading to increased K^+ currents at resting membrane potential (Kalappa et al., 2015; Tatulian et al., 2001). To generate KCNQ2/3 channel activators with increased potency and selectivity, we partitioned retigabine's chemical structure into three distinct zones (Figure 1). During the first round of chemical synthesis we mainly modified zones 1 and 3, whereas in the second iteration of our structure-activity relationship (SAR) analysis, we combined the beneficial modifications found for zones 1 and 3 with previously known beneficial modifications on zone 2, which led to the development of SF0034 (Figure 1, Kalappa et al., 2015). Based on the site of modification, we also categorized 1st generation compounds into three classes. Class I compounds had substitutions at the phenyl ring in zone 1, class II compounds had substitutions at the methylene group in zone 1, and class III compounds featured substitutions in zone 3 (Figure 2). Our guiding principle for this round of SAR studies was to modulate both steric and, in particular, electronic features in zone 1 by introducing fluoride, trifluoromethyl, and, importantly, a novel pentafluorosulfanyl group, which is considered a “super-trifluoromethyl” substituent (Alvarez et al., 2015; Mo et al., 2010; Wipf et al., 2009). These modifications led to our class I analogs NR561_29, NR561_40, NR561_45, and NR561_50. As part of our class II analog design, we introduced substituents at the benzylic methylene group, designed to slow down metabolic degradation (trifluoromethyl: NR579_04; deuterium: NR561_87). Moreover, we introduced a preliminary series of heterocycle analogs of the phenyl group in zone 1, i.e. a more electron-rich thiophene (NR579_46) and a more electron-deficient thiazole (NR579_38). Finally, our class III design modified the steric size of the ethylcarbamate in zone 3 by introducing an *iso*-propyl group (NR561_62) and the solubilizing

oxetane derivatives NR579_45 and NR579_36 (Skoda et al., 2014; Sprachman and Wipf, 2012; for synthesis details and spectroscopic information on these compounds, see supplemental data).

Incorporation of highly fluorinated substituents at the phenyl ring of retigabine increases the potency of KCNQ2/3 channel activation

To set the control conditions for assessing the potency and selectivity of the newly synthesized compounds, we first evaluated the ability of two standard activators, retigabine and SF0034, in potentiating KCNQ2/3 channel-mediated K⁺-currents under our assay conditions (Fig. 3). We transiently expressed heterologous KCNQ2/3 channels in CHO cells and tested the effect of increasing concentrations (100 nM to 30 μ M) of retigabine and SF0034 on KCNQ2/3 currents. We employed whole cell patch clamp electrophysiological techniques (Kalappa et al., 2015). 100 nM SF0034 increased KCNQ2/3 currents at hyperpolarized potentials, whereas 100 nM retigabine failed to show any effect (Fig. 3A₁, B₁). Consistent with our previous studies (Kalappa et al., 2015), SF0034 was approximately five times more potent than retigabine in shifting the V_{1/2} of KCNQ2/3 currents (Fig. 3A-D; retigabine: EC₅₀ 3.3 \pm 0.8 μ M, n=4-11; SF0034: EC₅₀ 0.60 \pm 0.06 μ M, n=5-21, *p* < 0.01).

Next, we tested the ability of the newly synthesized compounds to shift the V_{1/2} of KCNQ2/3 currents. We used different concentrations of these analogs to evaluate whether the new substituents resulted in gain or loss of potency in activating KCNQ2/3 currents compared to retigabine and SF0034. A concentration of 100 nM of NR561_40 (CF₃-group at the 4-position of the phenyl ring) increased the KCNQ2/3 currents at hyperpolarized potentials (Fig. 4A₁).

Consistent with this finding, a Boltzmann fit of the G-V relationship revealed a significant shift in the $V_{1/2}$ towards hyperpolarized potentials in the presence of 100 nM or 10 μ M NR561_40 without altering G_{\max} ($G_{\max, \text{nor}}$: control: 0.95 ± 0.015 ; n=9, 100 nM: 0.99 ± 0.043 ; n=5, 10 μ M: 0.97 ± 0.108 ; n=4) (Fig. 4A₂, A₃). Similarly, we measured the shift in $V_{1/2}$ in the presence of increasing concentrations of NR561_40 (100 nM - 30 μ M) and calculated the EC₅₀ values (Fig. 4A₄). NR561_40 showed a similar potency as SF0034 (Fig. 5A). Because retigabine has only one fluorine atom at the 4-position of the phenyl ring, these results suggested that increasing the steric bulk and electron-withdrawing properties at this position improves the potency at KCNQ2/3 channels. NR561_29, which has an even larger and more electronegative SF₅-group at this position, demonstrated a 4-5 fold higher potency compared to retigabine, but showed a significantly lower maximal $\Delta V_{1/2}$ compared to NR561_40 and SF0034, maximal $\Delta V_{1/2}$ values were calculated from the observed shift in $V_{1/2}$ at 10 μ M concentrations of the compound (Fig. 5B). This result suggested that a large steric size in zone 1 might limit the potency/efficacy at KCNQ2/3 channels (Fig. 5). Furthermore, when either the smaller CF₃-group or the larger SF₅-group were introduced at the 3-position of the phenyl ring, the resulting NR561_50 (Fig. 4B) and NR561_45, both showed similar potency but a lower maximal $\Delta V_{1/2}$ compared to NR561_40 and SF0034. From this result we concluded that the exact position of the fluorinated groups at the phenyl ring plays a critical role in determining the potency/efficacy of KCNQ activators at KCNQ2/3 channels.

Likewise, we tested class II and class III compounds for their potency and efficacy at shifting the $V_{1/2}$ of KCNQ2/3 currents. Class II compounds NR579_38, NR579_46 and NR561_87 shifted the $V_{1/2}$ of KCNQ2/3 channels, but did not show any improvement in EC₅₀ values relative to retigabine. Interestingly, NR579_04 failed to show any effect on KCNQ2/3 channel currents,

even at concentrations as high as 10 μ M, demonstrating the need for a small linker between the phenyl ring and the benzylic amine (Figs. 4C, 5). Among class III compounds, only NR561_62 demonstrated potency that was 2-3 fold better than retigabine; the more hydrophilic substituents were not tolerated (Fig. 4D). Taken together, our SAR results demonstrate that the position and the steric size of fluorinated groups in zone 1 of retigabine are critical determinants of compound potency and efficacy. Addition of CF₃- and SF₅-groups in positions 3 and 4 of the phenyl ring of retigabine generates KCNQ2/3 activators with increased potency over retigabine. Incorporation of a trifluoromethyl substituent specifically at the *para*-position of the benzylamine moiety resulted in the maximal improvement in potency and efficacy at KCNQ2/3 channels, eclipsing that of SF0034. Manipulation of the retigabine structure as probed in class II and III compounds did not provide further improvements in KCNQ2/3 channel potency, with the exception of NR561_62, where the ethyl group was replaced with a more lipophilic *iso*-propyl chain in the carbamate moiety.

KCNQ2/3 selectivity of CF₃- and SF₅-containing analogs

Next, we determined the selectivity profile of class I compounds that showed increased potency for KCNQ2/3 channels, i.e. NR561_40, NR561_50 and NR561_29. To assess the selectivity of these analogs, we quantified their effect on homomeric KCNQ4 and KCNQ5 channels. First, we tested NR561_50 at homomeric KCNQ4 channels. A concentration of 100 nM of NR561_50 failed to alter the $V_{1/2}$ of KCNQ4 channels (Fig. 6A₁). A Boltzmann fit of the G-V relationship in presence of 100 nM or 1 μ M compound did not shift the $V_{1/2}$ of KCNQ4 channels (Fig. 6A₂, A₃). Similarly, NR561_50 did not shift the $V_{1/2}$ of KCNQ5 channels (Fig. 6B). Although 100 nM NR561_40 and NR561_29 did not change the $V_{1/2}$, at 1 μ M concentration, both NR561_40 and

NR561_29 shifted the $V_{1/2}$ of KCNQ4 currents towards more hyperpolarized potentials (Fig. 6C, E). Furthermore, NR561_40 and NR561_29 increased KCNQ5 currents and shifted the $V_{1/2}$ to more hyperpolarized potentials at 100 nM and 1 μ M (Fig. 6D, F). Taken together, NR561_50 proved to be selective for KCNQ2/3 channels whereas NR561_40 and NR561_29 were found to be less selective. This profile suggests that incorporation of a trifluoromethyl group at the *meta*-position of the benzylamine generates activators with enhanced KCNQ2/3 selectivity.

Incorporation of a fluorine substituent in zone 2 in analogs with CF₃- and SF₅- functions in zone 1 generates the most potent KCNQ2/3 activator yet described

Because incorporation of a fluorine atom at the 3-position of the aniline ring of retigabine improved the potency and selectivity at KCNQ2/3 channels (Kalappa et al., 2015), we hypothesized that addition of fluorinated groups in zone 2 might also further improve the potency and selectivity of class I compounds. To test our hypothesis, we selected the most potent and efficacious compounds based on the 1st generation SAR (Fig. 5) and introduced a fluorine atom at the 3-position of the aniline. In this fashion, RL648_81 was obtained as the fluorinated analogue of NR561_40, RL648_73 as the fluorinated analogue of NR648_50, RL648_86 as the fluorinated analogue of NR561_62, and RL673_02 as the fluorinated analogue of NR561_45 (Fig. 7; for synthetic and spectroscopic details, see supplemental data).

We first evaluated the effect of different concentrations of RL648_81 at KCNQ2/3-mediated currents (Fig. 8A₁). Application of 100 nM RL648_81 robustly shifted the $V_{1/2}$ of KCNQ2/3 channels towards hyperpolarized potentials. Also, increased concentrations of 1 μ M or 10 μ M compound showed a more robust shift in $V_{1/2}$ compared to the shift caused by 1 μ M or 10 μ M

SF0034 (Fig. 8A2-A4). Evaluation of the EC_{50} revealed that RL648_81 is 3 times more potent than SF0034 at shifting the voltage dependence of KCNQ2/3 channels to more hyperpolarized potentials (Fig. 8D; EC_{50} $0.19 \pm 0.02 \mu\text{M}$, $n=5$). This shift in $V_{1/2}$ was not associated by changes in G_{max} (Fig. 8A1-3; $G_{\text{max:nor}}$: control: 0.96 ± 0.012 ; $n=9$, 100 nM: 1.01 ± 0.108 ; $n=5$, 01 μM : 1.01 ± 0.012 ; $n=4$, 10 μM : 0.95 ± 0.070 ; $n=4$). To assess the selectivity of RL648_81, we tested 100 nM, 1 μM and 10 μM of RL648_81 on homomeric KCNQ4 and KCNQ5 channel currents (Fig. 8B, C). RL648_81 did not shift the $V_{1/2}$ of either KCNQ4 or KCNQ5, suggesting that RL648_81 is a KCNQ2/3-specific activator (Fig. 8B, C).

Next, we evaluated RL648_76, RL648_86 and RL673_02 for their potency and selectivity at KCNQ2/3 channels. RL648_73 and RL648_86 showed 2-fold improved potency compared to SF0034 at KCNQ2/3 channels, whereas RL673_02 did not show a significant difference from SF0034, in agreement with the previously noted attenuation of potency with the sterically demanding SF_5 substituent (Fig. 8D left). These compounds, with the exception of the effect of 10 μM RL673_02 on KCNQ4 channels, also did not show any significant effect on either KCNQ4 or KCNQ5 channel currents (Fig. 8E, F).

The conserved residue, tryptophan (W) in the intracellular end of the S5 helix, W236 for KCNQ2 numbering and W265 for KCNQ3 numbering, is necessary for the enhancing effect of retigabine (Schenzer et al., 2005). To determine whether the gating effect of RL648_81 also requires the same W residue, we examined the influence of RL648_81 in KCNQ2 channels that lack W236. Indeed, although RL648_81 had a strong gating effect on KCNQ2 channels, this efficacy was abolished upon substitution of W236 to L (Fig. 9 A, B). These results suggest that RL648_81, like retigabine and SF0034, requires W236 to exert its enhanced gating properties.

MOL Manuscript #103200

Taken together, our SAR investigations led to the discovery of several highly selective and potent channel agonists, including the most potent KCNQ2/3-specific channel activator reported to date, RL648_81, which demonstrated three times higher potency than SF0034. Moreover, RL648_73 and RL648_86, which are two times more potent than SF0034, represent useful secondary lead compounds. ADME/tox data for SF0034 are not available yet, but in view of the undesired side effects associated with retigabine, we suggest that these more potent, selective and electronically deactivated KCNQ2/3 activators may be attractive candidates for treating or preventing hyperexcitability disorders at lower dosage and with reduced side effects.

Discussion

Epilepsy is a hyperexcitability disorder that affects approximately 65 million people worldwide (Bialer and White, 2010). Despite the availability of more than 20 antiepileptic drugs, 25-40% of epileptics are refractory to the treatment (Brodie, 2010). Moreover, even when currently available drugs are helpful, they are not without adverse effects (Bialer et al., 2010; Thurman et al., 2011). Therefore, there is an urgent need for novel drugs with improved therapeutic index characterized by increased potency and reduced toxicity.

Retigabine, which stabilizes the open state of KCNQ2-5 channels and shifts the voltage-dependence towards more hyperpolarized potentials (Wuttke et al., 2005), is an FDA approved KCNQ channel activator that serves as an add-on for the treatment of resistant partial-onset seizures (Gunthorpe et al., 2012). However, recently identified side effects of retigabine, including retinal abnormalities, skin discoloration and urinary retention, are significantly limiting its clinical use.

Here, we disclose the preparation and biological analysis of RL648_81 and related analogs, and report that this compound is the most potent KCNQ2/3-specific channel activator known to date. Due to its higher, yet selective agonism on KCNQ2/3 channels, RL648_81 is expected to be more effective at a lower dose than retigabine and its analog, SF0034, in preventing seizures. In addition, RL648_81 does not activate either KCNQ4 or KCNQ5. Because of its enhanced specificity over retigabine, RL648_81 is expected to have fewer side effects.

Although the mechanism by which retigabine-mediated toxicity influences skin and retina remains poorly understood, one hypothesis is that UV radiation may cause photodegradation and oxidation of retigabine's aniline ring, which may lead to the formation of colored deposits in skin and eyes. The incorporation of electron-withdrawing highly fluorinated substituents significantly

reduces the highest occupied molecular orbital energy of RL648_81 (-8.33 eV) vs. retigabine (-8.06 eV), and thus should render the former compound less prone to formation of reactive metabolites (Kawai et al., 2007). The trifluoromethylated RL648_81 is also expected to be more resistant to photodegradation and therefore less toxic to the eye and to the skin (Dow et al.; 2006). In particular, the electronic properties of RL648_81 (Fig. S2C) compared to retigabine (Fig. S2A) suggest that its aniline π -system as well as all three attached nitrogen atoms are considerably more electron-deficient. Furthermore, the CF₃-substituent is a stronger deactivator of the benzylamine π -system, and also presents a greater steric barrier to potential cytochrome P450-induced arene hydroxylation. The electrostatic potential map for RL673_02 (Fig. S2B) and RL648_73 (Fig. S2D) is closely related to that of RL648_81, with the SF₅-substituent in RL673_02 providing even greater steric and electronic deactivation of the compound.

The conserved residue W236 is necessary for the enhancing effect of retigabine, SF0034, and RL648_81 on the gating properties of KCNQ2 channels (Schenzer et al., 2005). Whereas it was thought that the critical property of W was its hydrophobicity (Wuttke et al., 2005), recent studies revealed that the ability of W to form H-bonds with the carbonyl/carbamate oxygen atom present in retigabine makes this contact critical (Kim et al., 2015). These studies suggest that the strength of the H-bond between retigabine and W236 determines the potency of retigabine. In part, the improved potency of SF0034 and RL648_81 is probably due to their ability to form stronger H-bonds with W236 than retigabine. However, besides W265, other residues are important for the gating effects of retigabine, such as L272, L314, and Leu-338 (KCNQ3 numbering) and G301/G340 (KCNQ2/KCNQ3 numbering) (Schenzer et al., 2005; Wuttke et al., 2005; Lange et al., 2009). Thus based on our SAR studies, we also suggest that the activity of analogs can be further modulated by hydrophobic interactions at the benzylamine moiety, which

the carbamate-W236 interaction positions into the vicinity of L272, L314, and L338 (Lange et al., 2008), and that the more lipophilic RL648_81 ($\log P=3.4$) is a better fit than retigabine ($\log P=2.5$) for this hydrophobic pocket at the pore-forming S5 inner loop and S6 helix domains, located near the intracellular voltage-operated gate of KCNQ2–5 channels.

In conclusion, our investigation of fluorinated substituents on retigabine, in particular the effect of highly fluorinated polar and lipophilic CF_3 - and SF_5 -groups in the benzylamine portion of the KCNQ2-5 channel activator, yielded a series of submicromolar affinity activators with exquisite selectivity for KCNQ2/3. We propose that the combination of increased potency and selectivity of RL648_81, as well as its structural features and modified electrostatic properties, may provide a solution to the problems associated with the undesirable side effects associated with retigabine.

MOL Manuscript #103200

Acknowledgements

We thank Dr. Anastassios Tzingounis for providing KCNQ2/3 mutants and Karen Hartnet for help with cell culture and plasmid preparation.

MOL Manuscript #103200

Authorship Contributions

Participated in research design: MK, PW, EA and TT

Conducted experiments: MK, NR, PW and RL

Contributed new reagents or analytic tools: RL, MK, and EA

Performed data analysis: MK, TT, RL, NR and PW

Wrote or contributed to the writing of the manuscript: MK, EA, PW, RL and TT

References

- Alvarez C, Arkin MR, Bulfer SL, Colombo R, Kovaliov M, LaPorte MG, Lim C, Liang M, Moore WJ, Neitz RJ, Yan Y, Yue Z, Huryn DM and Wipf P (2015) Structure–Activity Study of Bioisosteric Trifluoromethyl and Pentafluorosulfanyl Indole Inhibitors of the AAA ATPase p97. *ACS Medicinal Chemistry Letters* 6(12): 1225-1230.
- Bialer M, Johannessen SI, Levy RH, Perucca E, Tomson T and White HS (2010) Progress report on new antiepileptic drugs: a summary of the Tenth Eilat Conference (EILAT X). *Epilepsy research* 92(2-3): 89-124.
- Bialer M and White HS (2010) Key factors in the discovery and development of new antiepileptic drugs. *Nature reviews Drug discovery* 9(1): 68-82.
- Biervert C, Schroeder BC, Kubisch C, Berkovic SF, Propping P, Jentsch TJ and Steinlein OK (1998) A potassium channel mutation in neonatal human epilepsy. *Science (New York, NY)* 279(5349): 403-406.
- Brodie MJ (2010) Antiepileptic drug therapy the story so far. *Seizure* 19(10): 650-655.
- Brown DA and Adams PR (1980) Muscarinic suppression of a novel voltage-sensitive K⁺ current in a vertebrate neurone. *Nature* 283(5748): 673-676.
- Brown DA and Passmore GM (2009) Neural KCNQ (Kv7) channels. *British journal of pharmacology* 156(8): 1185-1195.
- Dalby-Brown W, Jessen C, Hougaard C, Jensen ML, Jacobsen TA, Nielsen KS, Erichsen HK, Grunnet M, Ahring PK, Christophersen P, Strobaek D and Jorgensen S (2013)

MOL Manuscript #103200

Characterization of a novel high-potency positive modulator of K(v)7 channels.
European journal of pharmacology 709(1-3): 52-63.

Davoren JE, Claffey MM, Snow SL, Reese MR, Arora G, Butler CR, Boscoe BP, Chenard L, DeNinno SL, Drozda SE, Duplantier AJ, Moine L, Rogers BN, Rong S, Schuyten K, Wright AS, Zhang L, Serpa KA, Weber ML, Stolyar P, Whisman TL, Baker K, Tse K, Clark AJ, Rong H, Mather RJ and Lowe JA, 3rd (2015) Discovery of a novel Kv7 channel opener as a treatment for epilepsy. *Bioorganic & medicinal chemistry letters* 25(21): 4941-4944.

Dow GS, Heady TN, Bhattacharjee AK, Caridha D, Gerena L, Gettayacamin M, Lanteri CA, Obaldia N, Roncal N, Shearer T, Smith PL, Tungtaeng A, Wolf L, Cabezas M, Yourick D, Smith,KS (2006) "Utility of alkylaminoquinolinyl methanols as new antimalarial drugs." *Antimicrob. Agents Chemother* 50, 4132-4143

Greenwood IA and Ohya S (2009) New tricks for old dogs: KCNQ expression and role in smooth muscle. *British journal of pharmacology* 156(8): 1196-1203.

Gribkoff VK (2008) The therapeutic potential of neuronal K V 7 (KCNQ) channel modulators: an update. *Expert opinion on therapeutic targets* 12(5): 565-581.

Grunnet M, Strobaek D, Hougaard C and Christophersen P (2014) Kv7 channels as targets for anti-epileptic and psychiatric drug-development. *European journal of pharmacology* 726: 133-137.

Gunthorpe MJ, Large CH and Sankar R (2012) The mechanism of action of retigabine (ezogabine), a first-in-class K⁺ channel opener for the treatment of epilepsy. *Epilepsia* 53(3): 412-424.

MOL Manuscript #103200

- Hansen HH, Waroux O, Seutin V, Jentsch TJ, Aznar S and Mikkelsen JD (2008) Kv7 channels: interaction with dopaminergic and serotonergic neurotransmission in the CNS. *The Journal of physiology* 586(7): 1823-1832.
- Howard RJ, Clark KA, Holton JM and Minor DL, Jr. (2007) Structural insight into KCNQ (Kv7) channel assembly and channelopathy. *Neuron* 53(5): 663-675.
- Iannotti FA, Barrese V, Formisano L, Miceli F and Taglialatela M (2013) Specification of skeletal muscle differentiation by repressor element-1 silencing transcription factor (REST)-regulated Kv7.4 potassium channels. *Molecular biology of the cell* 24(3): 274-284.
- Iannotti FA, Panza E, Barrese V, Viggiano D, Soldovieri MV and Taglialatela M (2010) Expression, localization, and pharmacological role of Kv7 potassium channels in skeletal muscle proliferation, differentiation, and survival after myotoxic insults. *The Journal of pharmacology and experimental therapeutics* 332(3): 811-820.
- Jankovic S and Ilickovic I (2013) The preclinical discovery and development of ezogabine for the treatment of epilepsy. *Expert opinion on drug discovery* 8(11): 1429-1437.
- Jentsch TJ (2000) Neuronal KCNQ potassium channels: physiology and role in disease. *Nature reviews Neuroscience* 1(1): 21-30.
- Kalappa BI, Soh H, Duignan KM, Furuya T, Edwards S, Tzingounis AV and Tzounopoulos T (2015) Potent KCNQ2/3-specific channel activator suppresses in vivo epileptic activity and prevents the development of tinnitus. *The Journal of neuroscience : the official journal of the Society for Neuroscience* 35(23): 8829-8842.

MOL Manuscript #103200

Kawai, M, Sakurada I, Morita A, Iwamuro Y, Ando K, Omura H, Sakakibara S, Masuda T, Koike H, Honma T, Hattori K, Takashima T, Mizuno K, Mizutani M, Kawamura M (2007) "Structure-activity relationship study of novel NR2B-selective antagonists with arylamides to avoid reactive metabolites formation." *Bioorg. Med. Chem. Lett.* 17, 5537-5542.

Kharkovets T, Hardelin JP, Safieddine S, Schweizer M, El-Amraoui A, Petit C and Jentsch TJ (2000) KCNQ4, a K⁺ channel mutated in a form of dominant deafness, is expressed in the inner ear and the central auditory pathway. *Proceedings of the National Academy of Sciences of the United States of America* 97(8): 4333-4338.

Kim RY, Yau MC, Galpin JD, Seebold G, Ahern CA, Pless SA and Kurata HT (2015) Atomic basis for therapeutic activation of neuronal potassium channels. *Nature communications* 6: 8116.

Lange W, Geißendorfer J, Schenzer A, Grotzinger J, Seebold G, Friedrich T, and Michael Schwake M (2008) Refinement of the Binding Site and Mode of Action of the Anticonvulsant Retigabine on KCNQ K_v Channels. *Molecular pharmacology* 75(2): 272-80.

Li S, Choi V and Tzounopoulos T (2013) Pathogenic plasticity of Kv7.2/3 channel activity is essential for the induction of tinnitus. *Proceedings of the National Academy of Sciences of the United States of America* 110(24): 9980-9985.

Li S, Kalappa BI and Tzounopoulos T (2015) Noise-induced plasticity of KCNQ2/3 and HCN channels underlies vulnerability and resilience to tinnitus. *eLife* 4.

MOL Manuscript #103200

- Li, Y., Gamper, N., Hilgemann, D.W. & Shapiro, M.S. (2005) Regulation of Kv7 (KCNQ) K⁺ channel open probability by phosphatidylinositol 4,5-bisphosphate. *The Journal of neuroscience : the official journal of the Society for Neuroscience*, **25**, 9825-9835.
- Miceli F, Soldovieri MV, Martire M and Taglialatela M (2008) Molecular pharmacology and therapeutic potential of neuronal Kv7-modulating drugs. *Current opinion in pharmacology* 8(1): 65-74.
- Mo T, Mi X, Milner EE, Dow GS and Wipf P (2010) Synthesis of an 8-pentafluorosulfanyl analog of the antimalarial agent mefloquine. *Tetrahedron Letters* 51(39): 5137-5140.
- Munro G and Dalby-Brown W (2007) Kv7 (KCNQ) channel modulators and neuropathic pain. *Journal of medicinal chemistry* 50(11): 2576-2582.
- Robbins J (2001) KCNQ potassium channels: physiology, pathophysiology, and pharmacology. *Pharmacology & therapeutics* 90(1): 1-19.
- Schenzer A, Friedrich T, Pusch M, Saftig P, Jentsch TJ, Grotzinger J and Schwake M (2005) Molecular determinants of KCNQ (Kv7) K⁺ channel sensitivity to the anticonvulsant retigabine. *The Journal of neuroscience : the official journal of the Society for Neuroscience* 25(20): 5051-5060.
- Sharma AK, Rani E, Waheed A and Rajput SK (2015) Pharmacoresistant Epilepsy: A Current Update on Non-Conventional Pharmacological and Non-Pharmacological Interventions. *Journal of epilepsy research* 5(1): 1-8.

MOL Manuscript #103200

Skoda EM, Sacher JR, Kazancioglu MZ, Saha J and Wipf P (2014) An uncharged oxetanyl sulfoxide as a covalent modifier for improving aqueous solubility. *ACS Med Chem Lett* 5(8): 900-904.

Soh H and Tzingounis AV (2010) The specific slow afterhyperpolarization inhibitor UCL2077 is a subtype-selective blocker of the epilepsy associated KCNQ channels. *Molecular pharmacology* 78(6): 1088-1095.

Sprachman MM and Wipf P (2012) A bifunctional dimethylsulfoxide substitute enhances the aqueous solubility of small organic molecules. *Assay and drug development technologies* 10(3): 269-277.

Stott JB, Jepps TA and Greenwood IA (2014) K(V)7 potassium channels: a new therapeutic target in smooth muscle disorders. *Drug discovery today* 19(4): 413-424.

Tatulian L, Delmas P, Abogadie FC and Brown DA (2001) Activation of expressed KCNQ potassium currents and native neuronal M-type potassium currents by the anti-convulsant drug retigabine. *The Journal of neuroscience : the official journal of the Society for Neuroscience* 21(15): 5535-5545.

Thurman DJ, Beghi E, Begley CE, Berg AT, Buchhalter JR, Ding D, Hesdorffer DC, Hauser WA, Kazis L, Kobau R, Kroner B, Labiner D, Liow K, Logroscino G, Medina MT, Newton CR, Parko K, Paschal A, Preux PM, Sander JW, Selassie A, Theodore W, Tomson T and Wiebe S (2011) Standards for epidemiologic studies and surveillance of epilepsy. *Epilepsia* 52 Suppl 7: 2-26.

Wickenden AD and McNaughton-Smith G (2009) Kv7 channels as targets for the treatment of pain. *Current pharmaceutical design* 15(15): 1773-1798.

MOL Manuscript #103200

- Wipf P, Mo T, Geib SJ, Caridha D, Dow GS, Gerena L, Roncal N and Milner EE (2009) Synthesis and biological evaluation of the first pentafluorosulfanyl analogs of mefloquine. *Organic & Biomolecular Chemistry* 7(20): 4163-4165.
- Wulff H, Castle NA and Pardo LA (2009) Voltage-gated potassium channels as therapeutic targets. *Nature reviews Drug discovery* 8(12): 982-1001.
- Wuttke TV, Seebohm G, Bail S, Maljevic S and Lerche H (2005) The new anticonvulsant retigabine favors voltage-dependent opening of the Kv7.2 (KCNQ2) channel by binding to its activation gate. *Molecular pharmacology* 67(4): 1009-1017.
- Xiong Q, Gao Z, Wang W and Li M (2008) Activation of Kv7 (KCNQ) voltage-gated potassium channels by synthetic compounds. *Trends in pharmacological sciences* 29(2): 99-107.

MOL Manuscript #103200

Footnotes

This work was supported by the Department of Defense, the Joint Warfighter Medical Research Program [W81XWH-14-1-0117] to T.T. and P.W..

Figure Legends

Figure 1. Zone SAR model of retigabine analogs.

Figure 2. Structure and classification of 1st generation compounds. Three classes of 1st generation KCNQ channel activators were synthesized based on our zone model. In class I and II, modifications were made in zone 1, in class III zone 3 was varied.

Figure 3. SF0034 is five-times more potent than retigabine in activating KCNQ2/3 channel currents. CHO cells transiently expressing heterologous KCNQ2/3 channels were clamped at -85 mV and KCNQ2/3 currents were elicited by 1 s depolarization step, in 10 mV increments, from -105 to +15 mV followed by return step to -70 mV; the voltage protocol is shown below A1. **A₁, B₁**, Representative current traces of KCNQ2/3 channels recorded at increasing membrane potentials in absence and presence of 100 nM retigabine (A₁) and 100 nM SF0034 (B₁). **A₂, B₂**, Representative curves of normalized G-V relationship of KCNQ2/3 currents at control and at increasing concentration of retigabine (A₂) and SF0034 (B₂). **C**, Summary bar graph representing half activation ($V_{1/2}$) of KCNQ2/3 currents calculated from normalized G-V Boltzmann curves at control and at increasing concentration of retigabine and SF0034. SF0034 at 100 nM significantly shifts the $V_{1/2}$ of KCNQ2/3 currents from control, whereas retigabine failed to show an effect at a 100 nM concentration. **D**, Representative curves showing the half activation shift ($\Delta V_{1/2}$) by retigabine with EC_{50} 3.3 ± 0.8 μ M (n=4-11, black) and SF004 with EC_{50} 0.60 ± 0.06 μ M (n=5-21, red) in a concentration dependent manner (100 nM – 30 μ M). Curves were fitted with a hill equation and EC_{50} values were calculated. Error bars represent

mean \pm SEM. $**p < 0.01$, $***p < 0.001$. Detailed values in supplemental data (Values for main figures).

Figure 4. Addition of a trifluoromethyl group at the 3- or 4-position of phenyl ring in zone 1 significantly increased the potency in activating KCNQ2/3 currents. CHO cells transiently expressing heterologous KCNQ2/3 channels were clamped at -85 mV and KCNQ2/3 currents were elicited by 1 s depolarization step, in 10 mV increments, from -105 to +15 mV followed by return step to -70 mV; the voltage protocol is shown below A1. **A-D₁**. Representative current traces of KCNQ2/3 channels recorded at increasing membrane potentials in absence and in presence of 100 nM NR561_40 (A₁), 100 nM NR561_50 (B₁), 100 nM NR579_04 (C₃) and 100 nM NR561_62 (D₁). **A-D₂**. Representative curves of normalized G-V relationship of KCNQ2/3 currents at control and at increasing concentration of NR561_40 (A₂), NR561_50 (B₂), NR579_04 (C₂) and NR561_62 (D₂). **A-D₃**. Summary bar graphs representing half activation ($V_{1/2}$) of KCNQ2/3 currents calculated from normalized G-V Boltzmann curves at control and at increasing concentration of NR561_40 (A₃), NR561_50 (B₃), NR579_04 (C₃) and NR561_62 (D₃). **A-D₄**. Representative curves showing half activation shift ($\Delta V_{1/2}$) by NR561_40 (EC_{50} 0.91 \pm 0.08 μ M, n=4-8; red) (A₄), by NR561_50 (EC_{50} 0.74 \pm 0.07 μ M, n=4-9; red) (B₄), by NR579_04 (EC_{50} NA, n=4-9; Red) (C₄) and by NR561_62 (EC_{50} 1.48 \pm 0.18 μ M, n=4-9; Red) (D₄). NR561_40 and NR561_50 showed similar potency as of SF0034 in activating KCNQ2/3 channel currents. NR561_62 showed 2-3 times lower potency than SF0034 whereas NR579_04 did not activate KCNQ2/3 currents at all. Curves were fitted with a hill equation and EC_{50} values were calculated. Error bars represent mean \pm SEM. $*p < 0.05$, $**p < 0.01$. Detailed values in supplemental data (Values for main figures).

Figure 5. Summary bar graphs representing (A) EC_{50} and (B) maximal (max) $\Delta V_{1/2}$ of first generation compounds tested at KCNQ2/3 channels. Like SF0034, first generation class I compounds NR561_40, NR561_50 and NR561_29 showed 4-5 times higher potency than retigabine in activating KCNQ2/3 channel currents. However, NR561_29 showed significant lower max $\Delta V_{1/2}$ compared to retigabine and SF0034. EC_{50} is the concentration of the compound that produces a half-maximal shift in $V_{1/2}$. Max $\Delta V_{1/2}$ is the shift in $V_{1/2}$ caused by 10 μ M of the tested compound. Detailed values in supplemental data (Values for main figures).

Figure 6. NR561_50 does not activate KCNQ4 and KCNQ5 channel currents. CHO cells transiently expressing heterologous homomeric KCNQ4 or KCNQ5 channels were clamped at -85 mV and currents were elicited by 1 s depolarization step, in 10 mV increments, from -105 to +15 mV followed by return step to -70 mV; the voltage protocol is shown below A1. **A₁, B₁** Representative current traces of KCNQ4 (A₁) and KCNQ5 (B₁) channels recorded at increasing membrane potentials in absence and in presence of 100 nM NR561_50. **A₂, B₂**. Representative curves of normalized G-V relationship of KCNQ4 (B₁) and KCNQ5 (B₂) currents at control, 100 nM and 1 μ M NR561_50. **A₃, B₃**. Summary bar graph representing half activation voltage ($V_{1/2}$) of KCNQ4 (A₃) and KCNQ5 (B₃) channel currents calculated from normalized G-V Boltzmann curves at control, 100 nM and 1 μ M NR561_50. **C₁, D₁**. Representative current traces of KCNQ4 (C₁) and KCNQ5 (D₁) channels recorded at increasing membrane potentials in absence and in presence of 100 nM NR561_40. **C₂, D₂**. Representative curves of normalized G-V relationship of KCNQ4 (C₂) and KCNQ5 (D₂) currents at control, 100 nM and 1 μ M NR561_40. **C₃, D₃**. Summary bar graph representing half activation voltage ($V_{1/2}$) of KCNQ4 (C₃) and KCNQ5 (D₃)

channel currents calculated from normalized G-V Boltzmann curves at control, 100 nM and 1 μ M NR561_40. **E₁, F₁** Representative current traces of KCNQ4 (E₁) and KCNQ5 (F₁) channel recorded at increasing membrane potentials in absence and in presence of 100 nM NR561_40. **E₂, F₂**. Representative curves of normalized G-V relationship of KCNQ4 (E₂) and KCNQ5 (F₂) currents at control, 100 nM and 1 μ M NR561_40. **E₃, F₃**. Summary bar graph representing half activation voltage ($V_{1/2}$) of KCNQ4 (E₃) and KCNQ5 (F₃) channel currents calculated from normalized G-V Boltzmann curves at control, 100 nM and 1 μ M NR561_40. Error bars represent mean \pm SEM. * p <0.05, ** p <0.01. Detailed values in supplemental data (Values for main figures).

Figure 7. Structures of 2nd generation compounds synthesized. Addition of a fluorine atom in zone 2 resulted in RL648_73, RL648_81, RL648_86, and RL673_02.

Figure 8. RL648_81 is three times more potent than SF0034 in activating KCNQ2/3 channel currents and does not potentiate KCNQ4 and KCNQ5 channel currents. CHO cells transiently expressing heterologous KCNQ2/3 channels or homomeric KCNQ4 and KCNQ5 channels were clamped at -85 mV and currents were elicited by 1 s depolarization step, in 10 mV increments, from -105 to +15 mV followed by return step to -70 mV; the voltage protocol is shown in A1 (left). **A₁**. Representative current traces of KCNQ2/3 channels recorded at increasing membrane potentials in absence and presence of 100 nM or 1 μ M RL648_81. **A₂**. Representative curves of normalized G-V relationship of KCNQ2/3 currents at control and at increasing concentration of RL648_81. **A₃**. Summary bar graph representing half activation ($V_{1/2}$) of KCNQ2/3 currents calculated from normalized G-V Boltzmann curves at control and at

increasing concentration of RL648_81 **A₄**. Representative curves showing half activation voltage shift ($\Delta V_{1/2}$) by RL648_81 (EC_{50} 0.19 ± 0.02 μ M, $n=4-11$; red) and SF0034 (EC_{50} 0.60 ± 0.06 μ M, $n=5-21$; black) in a concentration dependent manner (100 nM – 30 μ M). Curves were fitted with a hill equation and EC_{50} values were calculated. **B₁**. Representative current traces of KCNQ4 currents at increasing membrane potentials in absence and in presence of 100 nM RL648_81. **B₂**. Representative curves of normalized G-V relationship of KCNQ4 currents at control, 100 nM, 1 μ M and 10 μ M NR648_81. **B₃**. Summary bar graph representing half activation voltage ($V_{1/2}$) of KCNQ4 currents calculated from normalized G-V relationship curves at control, 100 nM, 1 μ M and 10 μ M RL648_81. **C₁**. Representative current traces of KCNQ5 currents at increasing membrane potentials absence and presence of 100 nM RL648_81. **C₂**. Representative curves of normalized G-V relationship of KCNQ5 currents at control, 100 nM, 1 μ M and 10 μ M NR648_81. **C₃**. Summary bar graph representing half activation voltage ($V_{1/2}$) of KCNQ5 currents calculated from normalized G-V Boltzmann curves at control, 100 nM, 1 μ M and 10 μ M RL648_81. **D**. Summary bar graphs representing EC_{50} and maximal $\Delta V_{1/2}$ values of second generation compounds tested at KCNQ2/3 channels in comparison with SF0034. RL648_73 and RL_86 showed 2 times higher potency than SF0034 in activating KCNQ2/3 channels. **E**. Summary bar graph representing half activation ($V_{1/2}$) of KCNQ4 currents calculated from normalized G-V Boltzmann curves in presence of 100 nM, 1 μ M and 10 μ M of RL648_73, RL648_86 and RL673_02. **F**. Summary bar graph representing half activation voltage ($V_{1/2}$) of KCNQ5 currents calculated from normalized G-V Boltzmann curves in presence of 100 nM, 1 μ M and 10 μ M of RL648_73, RL648_86 and RL673_02. Error bars represent mean \pm SEM. * p <0.05, *** p <0.001. Detailed values in supplemental data (Values for main figures).

Figure 9 Conserved residue tryptophan at S5 of KCNQ2-5 subunit is critical for potentiation effect of RL648_81 at KCNQ2 currents. CHO cells transiently expressing homomeric KCNQ2WT and KCNQ2(W236L) channels were clamped at -85 mV and currents were elicited by 1 s depolarization step, in 10 mV increments, from -105 to +15 mV followed by return step to -70 mV; the voltage protocol is shown below A1. **A₁, B₁**, Representative current traces of KCNQ2WT (A₁) and KCNQ2(W236L) (B₁) channels recorded at increasing membrane potentials in absence and presence of 10 μ M RL648_81. **A₂, B₂**, Representative curves of normalized G-V (conductance-voltage) relationship of KCNQ2WT (A₂) and KCNQ2(W236L) (B₂) currents at control and at increasing concentration of RL648_81. **C₁, C₂**, Summary bar graph representing half activation ($V_{1/2}$) of KCNQ2WT (C₁) and KCNQ2(W236L) (C₂) calculated from normalized G-V Boltzmann curves at control and at increasing concentration of RL648_81. Mutation of W236L at KCNQ2 subunit abolished the potentiation effect of RL648_81 at KCNQ2 currents. Error bars represent mean \pm SEM. * p <0.05, ** p <0.01. Detailed values in supplemental data (Values for main figures).

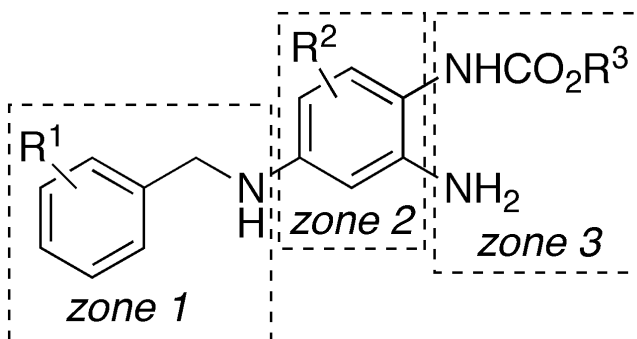
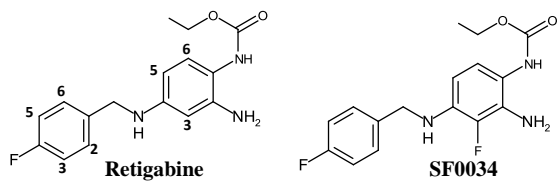
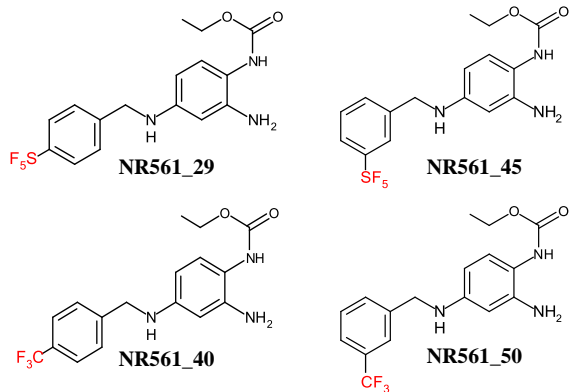


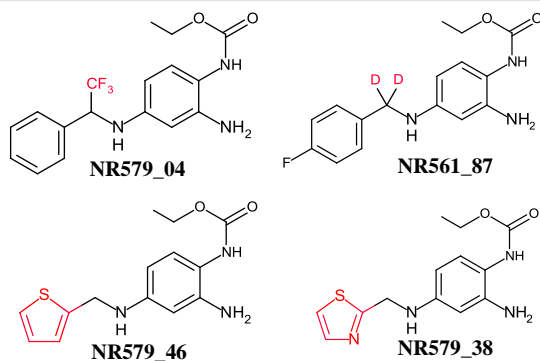
Figure 1.



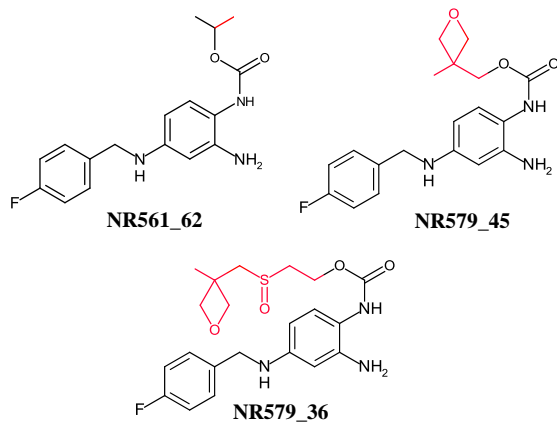
Parent Compounds



1ST Generation Class I



1ST Generation Class II



1ST Generation Class III

Figure 2.

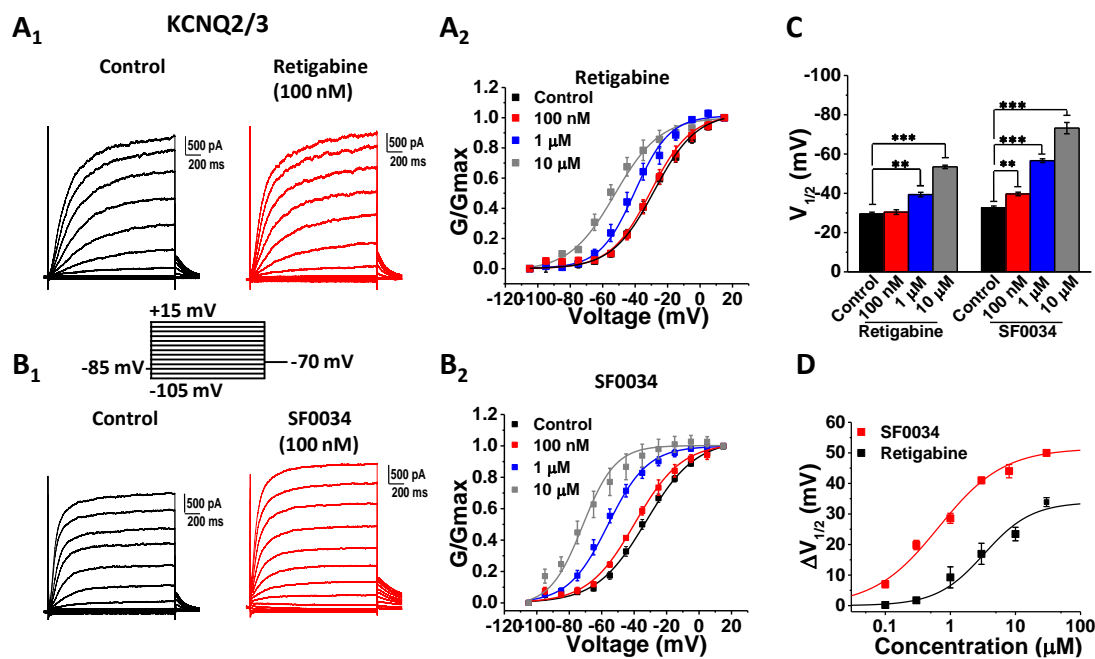


Figure 3.

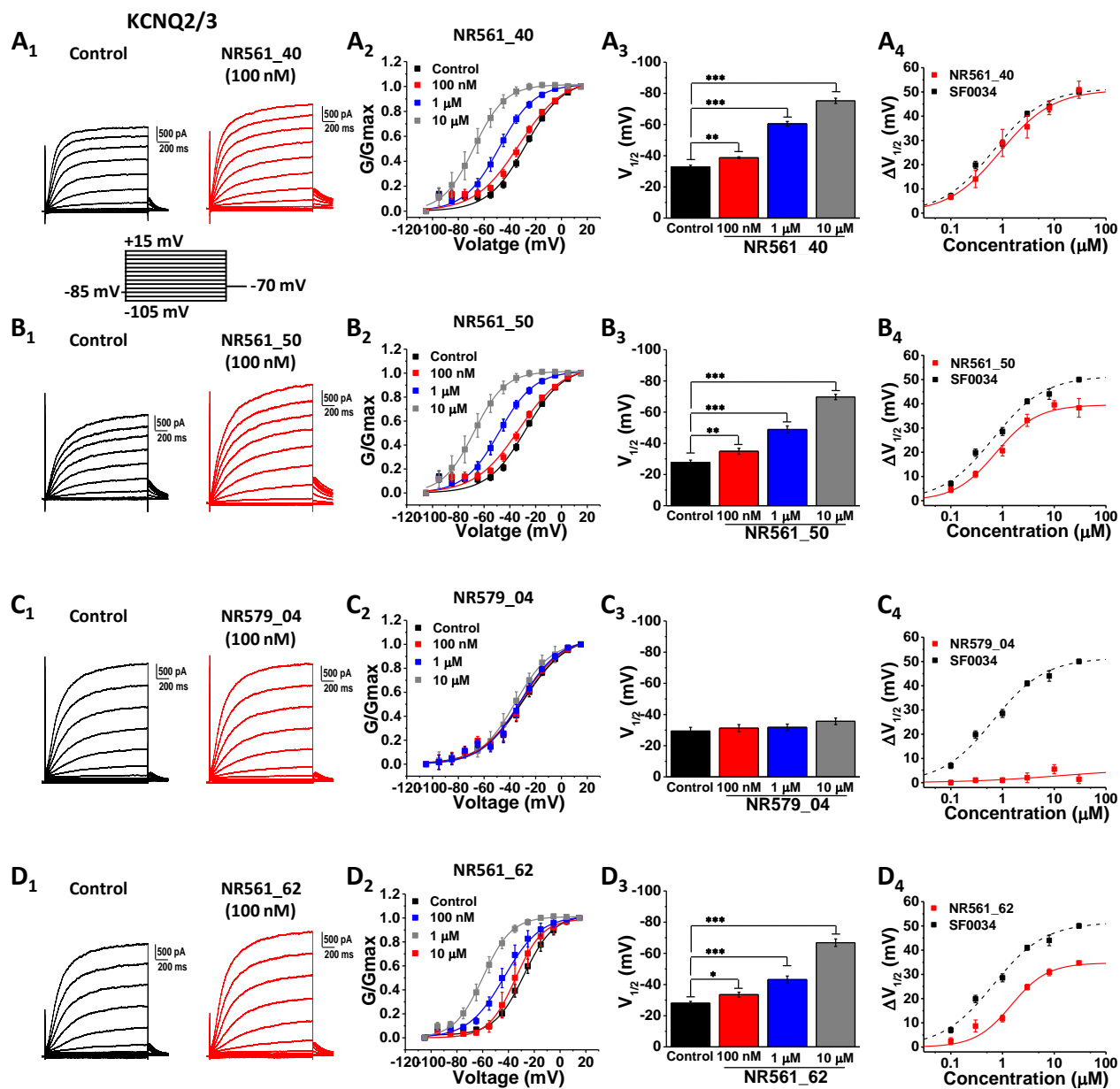


Figure 4.

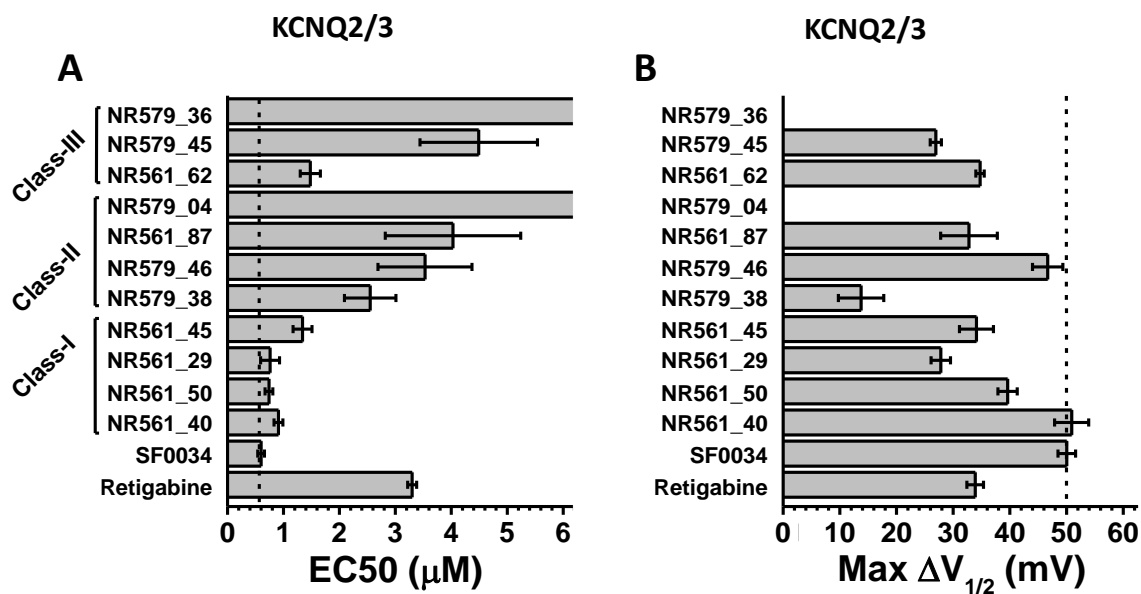


Figure 5.

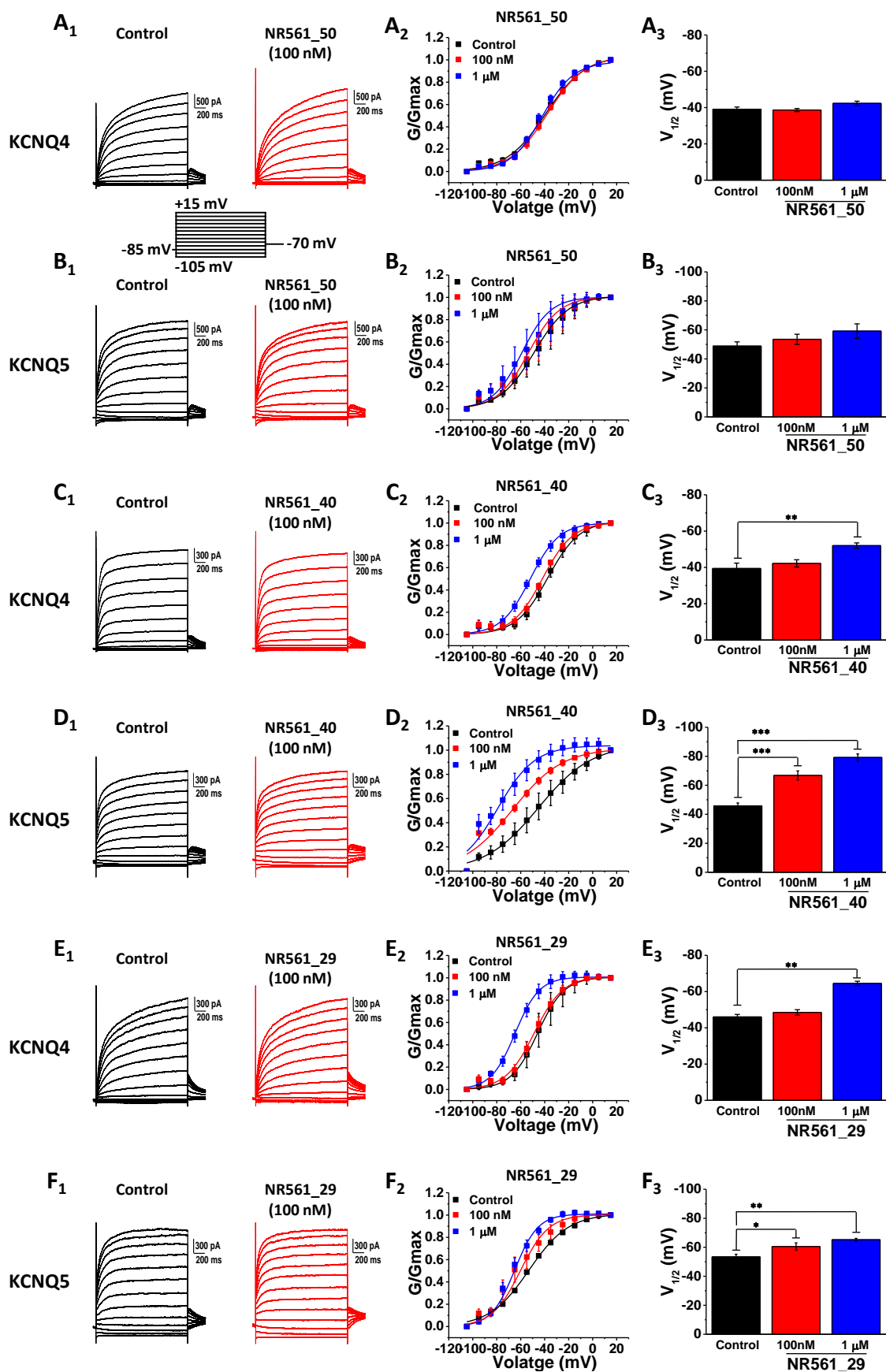


Figure 6.

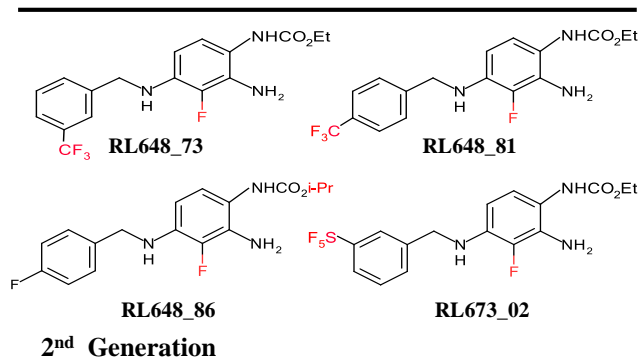


Figure 7.

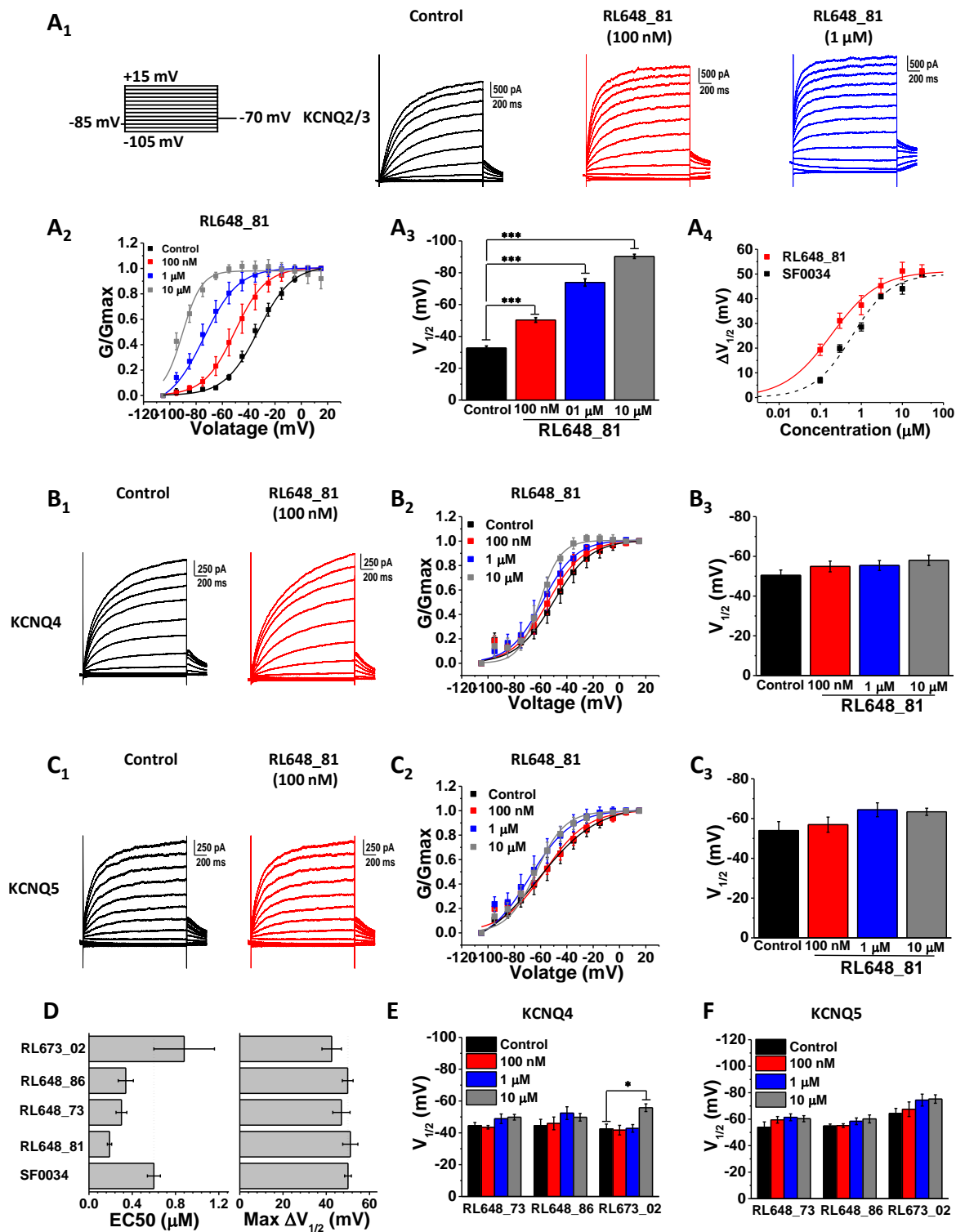


Figure 8.

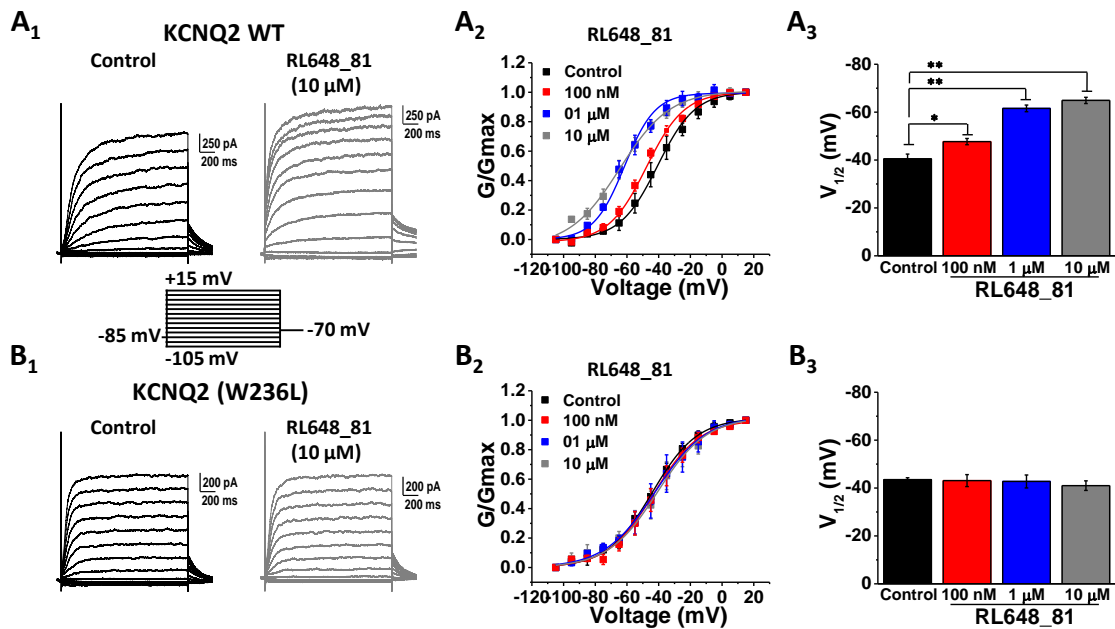


Figure 9.